Tunnelling and Underground Space Technology 74 (2018) 96–106

Contents lists available at ScienceDirect

Tunnelling and Underground Space Technology

journal homepage: www.elsevier.com/locate/tust

Elastic-slip interface effect on dynamic response of a lined tunnel in a semi-infinite alluvial valley under SH waves

Xue-Qian Fang*, Teng-Fei Zhang, Hai-Yan Li

Department of Engineering Mechanics, Shijiazhuang Tiedao University, Shijiazhuang 050043, China

A R T I C L E I N F O

Keywords:
Tunnel
Alluvial valley
Elastic-slip interface
Dynamic response

A B S T R A C T

A lined tunnel in a semi-infinite alluvial valley with an elastic-slip interface is constructed, and the dynamic stress distribution around the circular tunnel subjected to SH waves is analyzed. The elastic-slip interface model is introduced to simulate the actual interface condition. The Green's function is used to derive the wave fields of incident, scattered, and refracted waves. The elastic and slip coefficients are used to describe the interface properties. The displacement contours and dynamic stresses with different interface coefficients are analyzed. The interface effects under different wave frequencies and embedded depths are also examined in detail.

1. Introduction

Many irregular geological conditions such as alluvial valleys may significantly amplify ground movement resulting from the earthquakes. Consequently, concentrated damage to industrial and civil structures often occurs during earthquakes. Various numerical methods have been developed to study the response of alluvial valleys and underground structures, including the finite difference method (FDM) Chaillat et al., 2009, the finite element method (FEM) Najafizadeh et al., 2014; Bielak et al., 1991 and the boundary element method (BEM) Ba and Liang, 2017; Kawase and Aki, 1989.

In an alluvial valley, lined tunnels are usually built to pass through the valley. The irregular local geological topography may have a significant effect on the deformation and stress, and even initiate earthquakes (Bard and Bouchon, 1985; Dravinski, 1982; Luco and De Barros, 1994). Therefore, it is of great importance to predict the dynamic response of a field with special local geological conditions in earthquake resistance design. By employing Fourier–Bessel series expansion technique, the scattering and reflection of plane P waves by circular-arc alluvial valleys were described and the surface displacement was analyzed (Li et al., 2005). The boundary integral equation method was used to solve the site response of an alluvial valley or canyon under SH waves, and the half-plane radiation and scattering problems with circular boundaries were considered (Chen et al., 2008). A multi-domain indirect BEM was used to investigate SH wave scattering from a complex local site in a layered half-space (Ba and Yin, 2016). An indirect boundary integral equation method was introduced to solve the scattering of seismic waves by a three-dimensional layered alluvial basin (Liu et al., 2016). The seismic response of tunnel passing through an alluvial valley under SH waves was studied using the indirect-integral BEM, and the effects of wave frequency on the surface displacement and dynamic stress were discussed (Zhao et al., 2016). Based on the finite element method with a viscous-spring artificial boundary, formulas of equivalent nodal forces for plane P wave scattering with arbitrary incident angles were deduced and implemented into Abaqus (Huang et al., 2017). Alielahi and Adampira investigated the effects of an unlined tunnel (Alielahi et al., 2015) or two long unsupported parallel tunnels (Alielahi and Adampira, 2016) on the seismic response of the ground surface using the BEM in the time-domain. In their work, a linear elastic medium subjected to vertical SV and P waves was assumed. The time-domain BEM was also employed to predict site-effects of hill-cavity interaction subjected to SV and P waves. Significant effects of underground cavity and hill topography on the surface ground motion were found (Alielahi and Adampira, 2017).

In addition, a saturated porous medium was also introduced to simulate the surrounding medium, and Biot's dynamic theory was proposed. Based on Biot's dynamic theory, the diffraction of plane P-waves by a hemispherical alluvial valley was studied, and the effects of incident P-waves on the surface displacement amplitudes were discussed (Zhao et al., 2006). By introducing three potentials of Helmholtz equations and employing Biot's dynamic theory, the scattering of plane P waves by a circular-arc alluvial valley embedded in a poroelastic half-space was solved, and the stresses and pore pressures were analyzed (Zhou et al., 2008). By combining the method of fundamental solutions and Biot's dynamic theory, the diffraction of Rayleigh waves by a fluid-saturated poroelastic alluvial valley of arbitrary shape was investigated. The effects of alluvium porosity, valley shape, and incident frequency on the dynamic response were discussed in numerical examples (Liu

* Corresponding author.
E-mail address: stduxfang@yeah.net (X.-Q. Fang).

https://doi.org/10.1016/j.tust.2018.01.008
Received 3 September 2017; Received in revised form 25 December 2017; Accepted 5 January 2018

et al., 2016). The scattering of plane SV waves around a canyon embedded in a saturated poroelastic half-space was investigated by using the indirect boundary integrate equation method. The effects of incident frequency, soil porosity, boundary drainage condition, and canyon shape on the amplification effect of displacement were discussed (Liu et al., 2015). The scattering of plane fast compressional waves by a shallowly embedded tunnel in a poroelastic half-space was solved by using the indirect boundary integration equation method, and the amplification effect on the surface ground motion and the hoop stress in the tunnel was observed (Liu et al., 2017).

However, the above research mainly concerns the scattering of elastic waves around the local geological topography with perfect interfaces. Continuous displacements and stresses between the scattering bodies and the surrounding medium are assumed. This assumption simplifies the solution procedure. To simulate the actual interface, imperfect interface models such as a spring-type interface were proposed (Valier-Brasier et al., 2012; Fang et al., 2015). The imperfect interface effect on the strength was also found. In this interface model, the slip of the interface and the coupling of slip and elastic coefficients are ignored.

The purpose of this paper is to develop a new interface model to investigate the displacements and stresses around a circular tunnel embedded in a semi-infinite alluvial valley under SH waves. The elastic-slip interface model is used to simulate the actual interface condition. The boundary conditions around the tunnel become more complicated. A closed-form solution of SH wave scattering in the semi-infinite alluvial valley is presented using the Green's functions of the semi-infinite medium. Numerical solutions are obtained by discretising the boundaries of the tunnel and the alluvial valley. The displacement contour and dynamic stress distributions around the tunnel under different interface conditions are discussed.

2. Governing equations

Consider an alluvial valley existing in a semi-infinite space and a circular tunnel with infinite length embedded in the alluvial valley, as depicted in Fig. 1. The isotropic property of materials is assumed. The depth of the tunnel is d. The inner and outer radii of the tunnel are, respectively, denoted by a and b. The origin of the tunnel is o, and the coordinate system is shown in Fig. 1. 0An anti-plane wave with incident angle α propagates in the alluvial valley, as depicted in Fig. 2. The traction-free boundary condition at the semi-infinite surface is assumed. In this paper, the type of incident wave is oversimplified as SH waves. The incident wave field may be more complex than SH waves. The actual ground may behave as a three-dimensional structure, rather than a two-dimensional one. However, the closed-form solution of the two-dimensional structure can be derived in the following sections. If significant damping exists, surface waves cannot propagate over a large distance, so the damping of materials is neglected.

To simulate the imperfect interface around the tunnel, an elastic-slip interface model is developed, as shown in Fig. 1. In this model, an elastic spring in the radial direction and slip in the circumferential direction are introduced. The system is divided into three regions, i.e.,

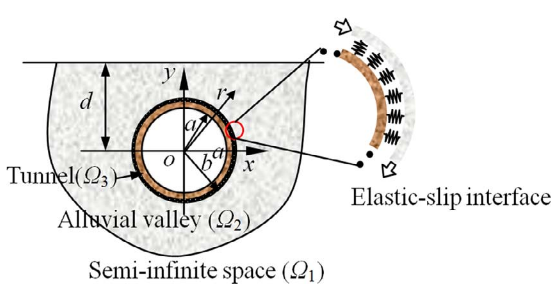

Fig. 1. A circular tunnel in semi-infinite alluvial valley and interface model.

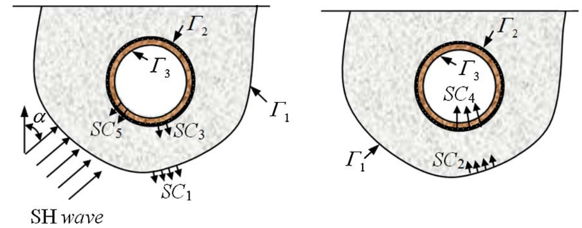

Fig. 2. Five scattering sources in the tunnel and alluvial valley.

Ω_1,Ω_2 and Ω_3.

The governing equation for the displacement W is expressed as (Pao and Mow, 1973)

$$\frac{\partial^2 W}{\partial x^2}+\frac{\partial^2 W}{\partial y^2}+k^2W=0, \tag{1}$$

where $k=\omega/c_{\rm SH}$ is the wave number of the anti-plane wave with ω being the incident frequency. $c_{\rm SH}=\sqrt{\mu/\rho}$ is the wave speed. ρ and μ are, respectively, the mass density and shear modulus of the medium.

The stresses resulting for the anti-plane displacement can be written as (Pao and Mow, 1973)

$$\tau_{xz}=\mu\frac{\partial W}{\partial x}\quad \tau_{yz}=\mu\frac{\partial W}{\partial y}, \tag{2}$$

where τ_{xz} and τ_{yz} are the shear stresses in the medium.

3. Wave fields in the regions

To obtain the total wave fields in the regions, the incident, scattered, and refracted waves should be given. Because of the existence of different regions, five scattering sources come into being, as depicted in Fig. 2. The outer and inner scattering waves at the boundary of the alluvial valley are denoted by SC_1 and SC_2, respectively. The outer and inner scattering waves at the interface between the tunnel and alluvial valley are denoted by SC_3 and SC_4, respectively. The scattering wave at the inner boundary of the tunnel is SC_5.

The displacement $W_{in}(x,y)$ of incident waves can be expressed as

$$W_{in}(x,y)=\exp[\mathrm{i}(k_xx+k_yy)]+\exp[\mathrm{i}(k_xx-k_yy)], \tag{3}$$

where $k_x=k\sin\alpha$, $k_y=k\cos\alpha$, and α is the incident angle of the SH waves. Subscript in denotes the incident waves and i= $\sqrt{-1}$.

To satisfy the traction-free boundary condition at the semi-infinite surface, the Green's functions of the semi-infinite medium for the displacements and stresses are expressed as (Kawase and Aki, 1989; Chen et al., 2008)

$$G(r,r_1)=\frac{\mathrm{i}}{4}(H_0^{(2)}(kr)+H_0^{(2)}(kr')), \tag{4}$$

$$\boldsymbol{T}(r,r_1)=\mu\left(\frac{\partial G(r,r_1)}{\partial n_x}+\frac{\partial G(r,r_1)}{\partial n_y}\right), \tag{5}$$

where $r\in\Omega_1$ and $r_1\in SC_1$. $H_0^{(2)}(\bullet)$ is the zero-th Hankel function of the second kind. n_x and n_y are the normal unit vectors corresponding to the $\boldsymbol{r}$ point in the scattering wave field. r' is the imaging point of $\boldsymbol{r}$ about the semi-infinite boundary. The larger argument in the complex Hankel function is introduced to ensure $H_0^{(2)}(\bullet)$ singularity and series convergence. To avoid the strong singularity at r', the image wave sources are deviated a certain distance.

Then, the displacement and stresses in the semi-infinite space (Ω_1) are expressed as

$$W_1(r)=\int_{SC_1}a(r_1)G(r,r_1)dSC_1, \tag{6}$$

$$\boldsymbol{\sigma}_1(r)=\int_{SC_1}a(r_1)\boldsymbol{T}(r,r_1)dSC_1, \tag{7}$$

where $a(r_1)$ is the density of the scattering wave source SC_1 at the point